CHEMISTRY
A EUROPEAN JOURNAL

DOI: 10.1002/chem.201202711

Photoswitchable Supramolecular Catalysis by Interparticle Host–Guest Competitive Binding

Liangliang Zhu,[a] Hong Yan,[a] Chung Yen Ang,[a] Kim Truc Nguyen,[a] Menghuan Li,[b] and Yanli Zhao*[a, b]

Supramolecular catalysts are of great interest because of their enzyme-like noncovalent interactions with substrates.[1] For example, some cyclodextrin dimers (bisCDs) and metallo-bisCDs have been used as supramolecular catalysts that are hydrolase mimics.[2] Generally, supramolecular catalysts are used homogeneously with respect to the substrates, and these catalysts cannot be recovered easily for reuse. Thus, effective and reversible immobilization methods[3] for the recovery of these catalysts are urgently needed. Although, chemists have investigated supramolecular catalysts by using in situ tuning of the reaction,[4] the development of switchable supramolecular catalysts that can be reversibly immobilized still remains a challenge.

We wanted to design and prepare supramolecular catalysts with the following attributes: 1) their activity can be switched on and off in situ by tuning competitive binding events, and 2) they contain an appropriate carrier that would allow reversible immobilization. CD–azobenzene dyads are the kernel of many light-driven artificial molecular machines, which have attracted a lot of attentions because of their intrinsic property to be controlled remotely without generating byproducts.[5] By taking advantage of the reversible assembly/disassembly of the CD host upon the *trans*–*cis* photoisomerization of the azobenzene guest, this dyad has been employed in the preparation of a variety of functional materials and devices, such as molecular switches,[6] molecular logic gates,[7] tunable soft materials,[8] responsive polymers,[9] nanoelectronics,[10] and drug-delivery systems.[11] Inspired by these developments, we propose to employ this phototriggerable host–guest binding process as the controllable inhibition process in supramolecular catalysis.

We chose gold nanoparticles (AuNPs) as the catalytic support onto which the CD-based supramolecular catalysts would be reversibly immobilized because (1) AuNPs can be easily prepared and isolated to serve as an effective heterogeneous nanocarrier and (2) the surface plasmon resonance (SPR) and the chromic property of AuNPs are sensitive to interparticle events;[12] these properties can be used either to indicate or monitor the switchable catalytic process. Thus, a key part of the preparation of the catalytic system is to graft azobenzene units onto the AuNP surface thus, placing the CD-based supramolecular catalysts between AuNPs through host–guest binding with the azobenzene units.

It has been well documented that the association constant for the binding of a β-CD ring with the *trans* isomer of azobenzene is greater than $10^3\,\mathrm{M}^{-1}$, indicating strong binding affinity within the dyad.[6–11] As a result, the CD-based supramolecular catalysts will initially encapsulate the *trans*-azobenzene units on the AuNP surface instead of the substrates for the catalytic reaction. Upon photoisomerization of the azobenzene unit from the *trans* to the *cis* form under UV-light irradiation, the binding affinity between the β-CD ring and the azobenzene unit will be weakened substantially, thus allowing the β-CD ring to encapsulate the reaction substrates and catalyze the transformation. When illuminating the system with visible light, the *cis*-to-*trans* photoisomerization of the azobenzene unit will cause the β-CD ring to form the inclusion complex with the *trans*-azobenzene unit, thus terminating the catalytic reaction again (Figure 1). Therefore, interparticle host–guest competitive binding was established .

To prepare the azobenzene-functionalized AuNPs, we first synthesized stable azobenzene-containing disulfide compound **L1** (Figure 1 and Figure S1 in the Supporting Information), the sulfide functionality being necessary for subsequent binding to the AuNPs. In its initial state, the azobenzene unit in compound **L1** adopts a *trans* conformation as evidenced by the ^{1}H NMR spectrum (see the Supporting Information, Figure S2 A). The *trans*-to-*cis* photoisomerization of the azobenzene unit occurs when the compound is irradiated by UV light at 365 nm. The presence of the *cis* isomer was confirmed by the ^{1}H NMR spectra, which shows a group of resonances in the aromatic region that are upfield shifted relative to those of the *trans* isomer (see the Supporting Information, Figure S2B). The maximum *trans*-to-*cis* photoisomerization efficiency is approximately 85 % accord-

---

[a] Dr. L. Zhu, Dr. H. Yan, C. Y. Ang, K. T. Nguyen, Prof. Dr. Y. Zhao
Division of Chemistry and Biological Chemistry
School of Physical and Mathematical Sciences
Nanyang Technological University
21 Nanyang Link, Singapore 637371
E-mail: zhaoyanli@ntu.edu.sg

[b] M. Li, Prof. Dr. Y. Zhao
School of Materials Science and Engineering
Nanyang Technological University
50 Nanyang Avenue, Singapore 639798

Supporting information for this article is available on the WWW under http://dx.doi.org/10.1002/chem.201202711.

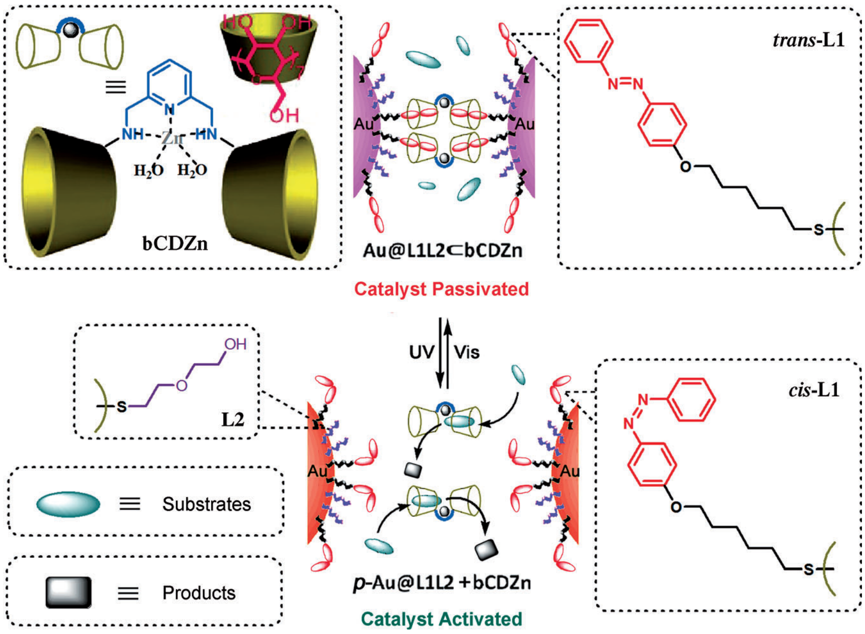

Figure 1. Structures of the supramolecular catalyst **bCDZn**, the ligand components, **L1** and **L2**, and a schematic representation of the phototriggered interparticle host–guest competitive binding for switchable catalysis. The stable catalytic states in this system are labeled as **Au@L1L2⊂bCDZn** and ***p*-Au@L1L2+bCDZn**. The proposed mechanism is also illustrated: the catalytic activity of **bCDZn** is passivated because the metallo-bisCDs are prone to bind with the *trans*-azobenzene unit of **L1** on the AuNP surface in preference to the substrates; upon photoisomerization of the *trans*-azobenzene unit to its *cis* isomer, dissociation of **bCDZn** from **L1** on the AuNPs readily occurs and allows **bCDZn** to bind with the substrates, thus leading to the activation of the catalytic reaction.

ing to the NMR-signal integration, an efficiency that is high relative to those of most other azobenzene derivatives[6–10] and ensures sufficiently efficient *trans*–*cis* interconversion on the nanoparticle surface. This photoisomerization is reversible and the *cis* isomer can be converted back into the *trans* isomer by irradiation using visible light (see the Supporting Information, Figure S2C).

Water-solubility is an essential prerequisite for the formation of CD–azobenzene complexes. Nevertheless, current approaches to impart hydrophilic character to azobenzene-containing disulfides are still relatively limited. Therefore, a mixed self-assembled monolayer (mSAM) strategy involving both **L1** and a hydrophilic ligand **L2** was employed to prepare water-soluble hybrid AuNPs. **L2** bears a polyethylene glycol moiety that has been proven to be unable to complex with the β-CD ring.[13] Upon optimization, an appropriate molar ratio (**L1**/**L2**=1:7, see the Supporting Information, Figure S3) facilitated the formation of an mSAM on the AuNP surface. The FT-IR spectrum of the functionalized AuNPs, **Au@L1L2**, shows a number of characteristic peaks (1500–1600 cm^{-1}) corresponding to the vibrations of aromatic moieties of compound **L1**, thus confirming the successful conjugation of **L1** onto the AuNP surface (see the Supporting Information, Figure S4). As **Au@L1L2** is well dispersed in water, a moderate Raman signal of **Au@L1L2** in aqueous solution was observed (see the Supporting Information, Figure S5). The thermal-stability investigation provided more detailed information on **Au@L1L2** (see the Supporting Information, Figure S6). Specifically, two distinct decomposition steps of **L1** were observed showing that this ligand undergoes substantial decomposition between 270 °C and 450 °C. The weight loss of **Au@L1L2** before it reaches 270 °C corresponds to the decomposition of **L2**, and the residue after 450 °C contributes to the inorganic Au core. Thus, we can deduce the average molar ratio between the attached azobenzene unit and the Au core to be approximately 2400:1.

Zn^{II}-coordinated pyridyl-bisCD (**bCDZn**), which is a highly efficient supramolecular catalyst for ester hydrolysis,[14] was employed to investigate host–guest binding with **Au@L1L2**. To ensure quantitative binding, we prepared an aqueous solution with a relatively high concentration of **Au@L1L2** (0.19 mM), and conducted all of the optical studies in a cuvette with a path length of 1 mm. Hybrid **Au@L1L2** has a characteristic SPR band at 524 nm (Figure 2 A, curve a); the TEM image (Figure 2 C) indicates that the nanoparticles are mainly monodispersed. To our delight, the SPR band underwent a bathochromic shift to 528 nm after the addition of 1 equivalent (relative to that of the azobenzene unit) of **bCDZn** (Figure 2 A, curve b). Subsequently, by introducing an excess amount of **bCDZn**, the band was further red-shifted to 530 nm (Figure 2 A, curves d and e). The positive signal at 360 nm in the induced circular dichroism (ICD) spectra confirms that the host–guest binding occurs (Figure 2 B), because the π–π* electronic transition of the azobenzene unit aligned parallel to the axis inside the CD cavity produces a positive Cotton effect.[15] Nanoparticle aggregates can be observed in the TEM image (Figure 2 D) at this stage, featuring interparticle host–guest binding. In addition, the solution color became deeper after the addition of **bCDZn** (see the inserts in Figure 2 C and 2D). For comparison purposes, control studies were conducted by the addition of pyridyl bisCD to the **Au@L1L2** solution and analyzing the resulting mixture by using UV/Vis and ICD studies. The positive ICD signal and the fact that the SPR band does not undergo a red-shift (see the Supporting Information, Figures S7 and S8) show that intraparticle host–guest binding rather than interparticle host–guest binding predominates. These data indicate that the Zn^{II}-coordinated rigid linkage between the two CD rings in **bCDZn** promotes interparticle host–guest binding (see

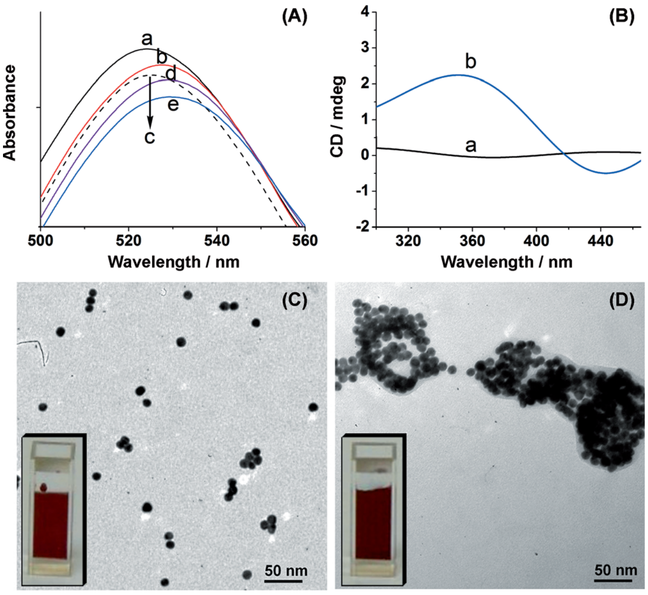

Figure 2. Formation of **Au@L1L2⊂bCDZn** and the phototriggered disassembly process in water at 298 K. (A) Absorption spectra (the SPR band) of (a) a solution of **Au@L1L2**, (b) a solution of **Au@L1L2** and 1 equiv of **bCDZn** (c) a solution of **Au@L1L2** and 1 equiv of **bCDZn** that has been photoirradiated using 365 nm UV light, (d) a solution of **Au@L1L2** and 10 equiv of **bCDZn** (e) a solution of **Au@L1L2** and 20 equiv of **bCDZn**. (B) Induced circular dichroism (ICD) spectra of (a) a solution of **Au@L1L2**, (b) a solution of **Au@L1L2** and 20 equiv of **bCDZn**. (C) TEM image of **Au@L1L2**. (D) TEM image of **Au@L1L2** after the addition of 20 equiv of **bCDZn**. The inserts in (C) and (D) shows the corresponding photographs of the solutions.

the schematic representation of **Au@L1L2⊂bCDZn** in Figure 1).

The hybrid **Au@L1L2** has excellent photochemical performance. Normally, illumination of **Au@L1L2** with a UV-light source with a wavelength of 365 nm and an intensity of 15 W for approximately 45 minutes is necessary for **Au@L1L2** to reach its photostationary state, ***p*-Au@L1L2**, where the azobenzene unit is in its *cis* form. Furthermore, the *trans–cis* photoswitching process of the azobenzene unit on **Au@L1L2** is reversible and repeatable by alternating between photoirradiation with 365 nm UV light and visible light (see the Supporting Information, Figure S9). Encouraged by the reversible photoswitching of the **Au@L1L2** hybrid, we proceeded to study the photoswitchability of **Au@L1L2⊂bCDZn**. The SPR band of **Au@L1L2⊂bCDZn** was blue-shifted after sufficient irradiation at 365 nm (Figure 2 A, curve c), thus indicating phototriggered disassembly of the CD–azobenzene complex followed by the redispersion of the AuNPs (see the schematic representation of ***p*-Au@L1L2+bCDZn** in Figure 1). Therefore, the **bCDZn** catalyst can be released from the nanoparticles by the *trans*-to-*cis* photoisomerization of the azobenzene unit, a process that is indicated by SPR band shifts.

To determine whether the catalytic activity of the system is photoswitchable, 4-nitrophenyl acetate (NA) and bis(4-nitrophenyl) carbonate (BNPC) were selected as catalytic-hydrolysis substrates because of their suitable structural features.[2,14] Before studying the kinetics of the hydrolysis, we needed to clarify the effect of the thermal isomerization[6a,16] of the azobenzene unit on AuNPs. Even at room temperature, the *cis*-azobenzene unit gradually converts back into the corresponding *trans* isomer in the dark. The apparent rate constant ($k = 0.0019\,\text{min}^{-1}$, first-order exponential growth fitting) for the recovery process was calculated in accordance with the changes of the π–π^* band (see the Supporting Information, Figure S10). Fortunately, one of the isoabsorptive points at 420 nm (see the Supporting Information, Figure S10 A) overlaps with the absorption band of the hydrolyzate, 4-nitrophenolate.[17] Therefore, the UV/Vis signal at 420 nm ($\varepsilon = 7130\,\text{M}^{-1}\,\text{cm}^{-1}$) was used to monitor the catalyzed hydrolysis reactions. The absorption of the catalysts at this wavelength was subtracted from the overall absorbance at this wavelength to compare the relative rates of hydrolysis (Figure 3). In addition, we only used **Au@L1L2** complexed with 1 equivalent of **bCDZn** in the catalytic study, because free **bCDZn** may interfere with the switchable catalysis.

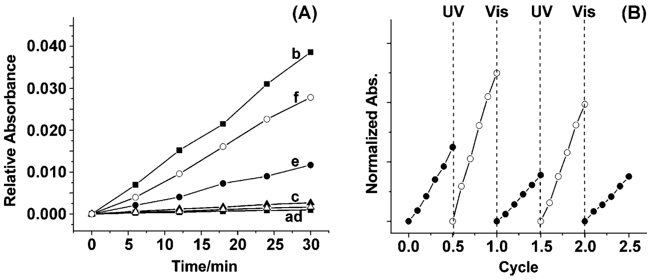

Figure 3. Switchable supramolecular catalysis for the hydrolysis of NA. (A) Plots of relative absorbance at 420 nm versus reaction time during the hydrolysis of NA in aqueous solution at 298 K: (a) without catalyst; (b) in the presence of **bCDZn**; (c) in the presence of **Au@L1L2**; (d) in the presence of ***p*-Au@L1L2**; (e) in the presence of **Au@L1L2⊂bCDZn**; (f) in the presence of ***p*-Au@L1L2+bCDZn**. (B) Normalized absorption changes at 420 nm during an ongoing hydrolysis process with photoirradiation for several cycles. Each cycle lasts 150 min. In each cycle, the solution is irradiated with visible light for 45 min and then its absorbance is measured for 30 min, followed by irradiation with 365 nm UV light for 45 min and the absorption measurement for another 30 min.

The initial rate of spontaneous hydrolysis of NA (1.9 mM) was relatively slow; the rate increased by approximately 40-fold in the presence of **bCDZn** (0.19 mM of the β-CD ring, 0.1 equivalent with respect to the substrate, see curves a and b in Figure 3 A). This rate enhancement can be attributed to the formation of a complex between the catalyst, **bCDZn**, and the substrate, an interaction that facilitates hydrolysis.[2,14] The presence of either **Au@L1L2** or its photostationary state ***p*-Au@L1L2** alone does not catalyze this reaction, as evidenced by the lack of obvious hydrolysis-rate enhancements (Figure 3 A, curves c and d).

Switchable catalysis was observed when NA was treated with composite **Au@L1L2⊂bCDZn**. There is only a small enhancement in the hydrolysis rate in the presence of **Au@L1L2⊂bCDZn** (Figure 3 A, curve e) because the β-CD rings of the catalyst **bCDZn** are occupied by the *trans*-azobenzene units on the AuNP surface. However, when the composite was converted into its photostationary state, ***p*-Au@L1 L2+bCDZn**, upon its irradiation with UV light, an approximate 30-fold enhancement in the hydrolysis rate was observed (Figure 3 A, curve f), which is close to enhancement observed when NA is treated with **bCDZn** (Figure 3 A, curve b). These data suggest that a photoinduced disassembly process leading to the release of **bCDZn** and ***p*-Au@L1 L2** is operating, the former then being free to catalyze the hydrolysis reaction. The switched-on catalytic activity is similar to that of a control experiment in which NA is treated with a water-soluble homogeneous system consisting of an azobenzene derivative and **bCDZn** (see the Supporting Information, Figure S11). Because the timescale of the hydrolysis of NA is generally longer than that of the photoisomerization of **Au@L1 L2⊂bCDZn**, the progress of the reaction can be either be impeded or promoted as required by irradiation of the reaction mixture with visible and UV light, respectively. This photoswitching of catalysis can be observed from the increase and the decrease of the hydrolysis rate with irradiation alternating between UV and visible light, respectively (Figure 3 B).

In contrast to the hydrolysis of NA, the hydrolysis of BNPC (0.95 mM) involves a two-step process.[18] For the first step, which is indicated by a decrease in the intensity of the UV/Vis signal at 280 nm (where BNPC absorbs), switchable catalysis was not observed (see the Supporting Information, Figure S12), simply because the binding affinity of BNPC to the β-CD dimers is relatively strong[19] and the azobenzene unit cannot effectively replace BNPC from the β-CD cavity. In contrast, this binding process does not occur for substrates containing only one phenyl group. The switching effect could be observed when monitoring the absorption of 4-nitrophenolate at 420 nm, the species that is formed during the second step of the hydrolysis reaction (see the Supporting Information, Figure S13). The apparent rates of hydrolysis of NA and BNPC in the presence of the different species were calculated (Table 1). In particular, the rates of the hydrolysis reactions catalyzed by **Au@L1 L2⊂bCDZn** and ***p*-Au@L1 L2+bCDZn** reveal significant differences in the catalytic activity of the composite when the azobenzene unit is in its *trans*- and *cis*-configured form. By comparing the apparent rate constants (see the Supporting Information), we concluded that the differences in the hydrolysis rates originate mainly from the amount of free **bCDZn** in solution. There is more **bCDZn** available for catalysis when the azobenzene unit undergoes the *trans*-to-*cis* photoisomerization on the AuNP surface.

Table 1. The rate of hydrolysis of NA and BNPC as catalyzed by different species.

Entry	Substrate	Catalyst	Rate (×10^{-8}) [M min^{-1}]
1	NA	none	4.52±0.32
2	NA	**bCDZn**	178±4.2
3	NA	**Au@L1 L2**	12.2±0.45
4	NA	***p*-Au@L1 L2**	7.65±0.87
5	NA	**Au@L1 L2⊂bCDZn**	54.1±1.9
6	NA	***p*-Au@L1 L2+bCDZn**	132±4.6
7	BNPC	none	null[a]
8	BNPC	**bCDZn**	334±12.9
9	BNPC	**Au@L1 L2**	null
10	BNPC	***p*-Au@L1 L2**	null
11	BNPC	**Au@L1 L2⊂bCDZn**	190±11.4
12	BNPC	***p*-Au@L1 L2+bCDZn**	250±16.2

[a] null means that the reaction is too slow to be measured accurately.

In summary, photoswitchable supramolecular catalysis of ester hydrolysis has been achieved using host–guest competitive binding of a Zn^{II}-coordinated β-cyclodextrin dimer catalyst with azobenzene units on the surfaces of gold nanoparticles in the presence of reaction substrates. When the β-cyclodextrin rings are occupied by the *trans*-azobenzene units, the catalyst no longer recognizes the substrate and therefore its catalytic activity is passivated. After the *trans*-to-*cis* photoisomerization of the azobenzene unit on the gold nanoparticle surface under UV irradiation, the azobenzene units are unable to bind with the β-cyclodextrin rings as tightly and thus the catalyst becomes available for catalyzing the hydrolysis of the substrates. We have also demonstrated that the catalytic process can be switched on and off repeatedly by alternating between UV- and visible-light irradiation. Because the host–guest competitive binding described here is an interparticle process, the switchable supramolecular catalyst can be reversibly immobilized on the gold nanoparticle surface, a process that can be followed by observing the changes to the SPR band of the gold nanoparticles. The results herein are valuable for the design and preparation of the next generation of catalytic materials with facile control over immobilization and catalytic activity.

Experimental Section

Synthesis of the compound **L1**: [4-[(6-Bromohexyl)oxy]phenyl]phenyldiazene (**A**)[20] (0.87 g, 2.4 mmol) and hexamethyldisilathiane (0.52 g, 0.61 mL, 2.9 mmol) were dissolved in dry THF (20 mL). The solution was cooled down to between 0 and 5 °C and a solution of TBAF (1 M) in THF (2.66 mL, 2.66 mmol) was then added. After the solution was warmed up to room temperature over 1.5 h, aqueous saturated ammonium chloride (50 mL) was added. The solid precipitates were collected by filtration and purified using silica gel chromatography (petroleum ether/ethyl acetate=9:2) to obtain compound **L1** (282 mg, 37.4 %). mp. 106–109 °C. ^{1}H NMR (400 MHz, $CDCl_3$, 298 K) δ=7.90 (m, 8 H), 7.49 (m, 6 H), 7.02 (d, J=9.0 Hz, 4 H), 4.06 (t, J=6.4 Hz, 4 H), 2.74 (t, J=6.8 Hz, 4 H), 1.84 (m, 4 H), 1.74 (m, 4 H), 1.55 (m, 8 H). ^{13}C NMR (100 MHz, $CDCl_3$, 298 K) δ=161.70, 152.84, 146.91, 130.33, 129.04, 124.77, 122.55, 114.70, 68.16, 38.97, 29.10, 28.69, 28.23, 25.75. HRMS (ESI) m/z: $[M+H]^+$ calcd for $C_{36}H_{43}N_4O_2S_2$, 627.2827; found m/z, 627.2830.

Compound **L2** was prepared using a procedure described in the literature.[21]

Synthesis of **bCDZn**: $Zn(NO_3)_2\cdot 6H_2O$ (40 mg, 0.134 mmol) was added to a stirred solution of pyridyl bisCD (**bCD**)[14] (202 mg, 0.085 mmol) in water (5 mL) at 45 °C. The resulting solution was stirred for another 6 h, and then the mixture was concentrated under reduced pressure. Ethanol (5 mL) was added to form precipitates, which were collected by filtration and washed with ethanol. The sample was dried in vacuo to give **bCDZn** (175 mg, 70.8 %) as a white solid. mp. 234–235 °C (decomp.). ^{1}H NMR (400 MHz, D_2O, 298 K) δ=7.95 (t, J=7.6 Hz, 1 H), 7.39 (d, J=8.0 Hz, 2H), 5.08–4.96 (m, 14H), 4.14 (m, 4H), 4.01–3.76 (m, 56H), 3.64–3.38 (m, 28H). ^{13}C NMR (100 MHz, D_2O, 298 K, δ): 153.44, 141.72, 122.30, 101.80, 101.40, 83.90, 81.12, 73.10, 72.03, 71.82, 68.15, 60.35, 50.17, 48.82. MS (ESI) m/z: $[M-2H_2O]^{2+}$ calcd 1216.87; found m/z, 1216.92. m/z: $[M+2H_2O]^{2+}$ calcd 1252.90; found m/z, 1253.25.

Citrate-stabilized AuNPs with an average diameter of 13 nm were prepared using a procedure described in the literature.[22]

Preparation of **Au@L1 L2**: The hybrid gold nanoparticles were prepared using a ligand-exchange reaction. Typically, 4 drops of a DMF solution of **L2** (0.29 M) were added into stirred citrate-stabilized AuNP aqueous solution (6 mL, 8.5 nM of gold spheres) in an 8-mL cleaned vial. The solution gradually turns colorless after approximately 30 mins. Then 4 drops of a DMF solution of **L1** (0.042 M) were added to the solution and stirring was continued for another 16 h, during which the solution turns red. Excess **L1** was removed by centrifugation (2500 rps, 23 min). The hybrid AuNPs were collected by centrifugation (6000 rps, 60 min) from the resulting solution and washed with deionized H_2O twice. Normally, the hybrid **Au@L1 L2** was stored in aqueous solution, which was concentrated for studies.

Acknowledgements

This work was financially supported by the Singapore National Research Foundation Fellowship (NRF2009NRF-RF001—015) and Nanyang Technological University. L.L.Z. thanks S.-J. Wu, Dr. P. -Z. Li, X. Li, and P. Borah for helpful discussions.

Keywords: azo compounds · cyclodextrins · gold nanoparticles · photoisomerization · supramolecular chemistry

---

[1] a) J. Meeuwissen, J. N. H. Reek, *Nat. Chem.* **2010**, *2*, 615–621 and references therein; b) P. W. N. M. van Leeuwen, D. Rivillo, M. Raynal, Z. Freixa, *J. Am. Chem. Soc.* **2011**, *133*, 18562–18565; c) H. J. Yoon, J. Kuwabara, J.-H. Kim, C. A. Mirkin, *Science* **2010**, *330*, 66–69; d) M. C. Feiters, A. E. Rowan, R. J. M. Nolte, *Chem. Soc. Rev.* **2000**, *29*, 375–384; e) L. Marinescu, M. Bols, *Curr. Org. Chem.* **2010**, *14*, 1380–1398.

[2] a) R. Breslow, S. D. Dong, *Chem. Rev.* **1998**, *98*, 1997–2011; b) R. Breslow, B. Zhang, *J. Am. Chem. Soc.* **1994**, *116*, 7893–7894; c) Z. Dong, X. Li, K. Liang, S. Mao, X. Huang, B. Yang, J. Xu, J. Liu, G. Luo, J. Shen, *J. Org. Chem.* **2007**, *72*, 606–609; d) Y.-H. Zhou, M. Zhao, Z.-W. Mao, L.-N. Ji, *Chem. Eur. J.* **2008**, *14*, 7193–7201.

[3] a) R. Palkovits, D. Arlt, H. Stepowska, F. Schüth, *Chem. Eur. J.* **2009**, *15*, 9183–9190; b) M. Tada, Y. Akatsuka, Y. Yang, T. Sasaki, M. Kinoshita, K. Motokura, Y. Iwasawa, *Angew. Chem.* **2008**, *120*, 9392–9395; *Angew. Chem. Int. Ed.* **2008**, *47*, 9252–9255; c) L. Wu, Y.-M. He, Q.-H. Fan, *Adv. Synth. Catal.* **2011**, *353*, 2915–2919; d) G. Liu, H. He, J. Wang, *Adv. Synth. Catal.* **2009**, *351*, 1610–1620.

[4] a) J. Wang, B. L. Feringa, *Science* **2011**, *331*, 1429–1432; b) O. B. Berryman, A. C. Sather, A. Lledó, J. Rebek Jr., *Angew. Chem.* **2011**, *123*, 9572–9575; *Angew. Chem. Int. Ed.* **2011**, *50*, 9400–9403; c) W.-S. Lee, A. Ueno, *Macromol. Rapid Commun.* **2001**, *22*, 448–450; d) R. Cacciapaglia, S. Di Stefano, L. Mandolini, *J. Am. Chem. Soc.* **2003**, *125*, 2224–2227; e) V. Blanco, A. Carlone, K. D. Hänni, D. A. Leigh, B. Lewandowski, *Angew. Chem.* **2012**, *124*, 5256–5259; *Angew. Chem. Int. Ed.* **2012**, *51*, 5166–5169.

[5] a) V. Balzani, A. Credi, M. Venturi, *Chem. Soc. Rev.* **2009**, *38*, 1542–1550; b) S. Silvi, M. Venturi, A. Credi, *Chem. Commun.* **2011**, *47*, 2483–2489; c) H. Li, A. C. Fahrenbach, A. Coskun, Z. Zhu, G. Barin, Y. L. Zhao, Y. Y. Botros, J.-P. Sauvage, J. F. Stoddart, *Angew. Chem.* **2011**, *123*, 6914–6920; *Angew. Chem. Int. Ed.* **2011**, *50*, 6782–6788.

[6] a) H. Murakami, A. Kawabuchi, R. Matsumoto, T. Ido, N. Nakashima, *J. Am. Chem. Soc.* **2005**, *127*, 15891–15899; b) L. Zhu, D. Zhang, D. Qu, Q. Wang, X. Ma, H. Tian, *Chem. Commun.* **2010**, *46*, 2587–2589; c) L. Zhu, M. Lu, D. Qu, Q. Wang, H. Tian, *Org. Biomol. Chem.* **2011**, *9*, 4226–4233.

[7] a) D. H. Qu, Q. C. Wang, H. Tian, *Angew. Chem.* **2005**, *117*, 5430–5433; *Angew. Chem. Int. Ed.* **2005**, *44*, 5296–5299; b) D. H. Qu, F. Y. Ji, Q. C. Wang, H. Tian, *Adv. Mater.* **2006**, *18*, 2035–2038.

[8] a) S. Tamesue, Y. Takashima, H. Yamaguchi, S. Shinkai, A. Harada, *Angew. Chem.* **2010**, *122*, 7623–7626; *Angew. Chem. Int. Ed.* **2010**, *49*, 7461–7464; b) X. Liao, G. Chen, X. Liu, W. Chen, F. Chen, M. Jiang, *Angew. Chem.* **2010**, *122*, 4511–4515; *Angew. Chem. Int. Ed.* **2010**, *49*, 4409–4413; c) Y. Wang, N. Ma, Z. Wang, X. Zhang, *Angew. Chem.* **2007**, *119*, 2881–2884; *Angew. Chem. Int. Ed.* **2007**, *46*, 2823–2826; d) Y. L. Zhao, J. F. Stoddart, *Langmuir* **2009**, *25*, 8442–8446; e) H. Jin, Y. Zheng, Y. Liu, H. Cheng, Y. Zhou, D. Yan, *Angew. Chem.* **2011**, *123*, 10536–10540; *Angew. Chem. Int. Ed.* **2011**, *50*, 10352–10356.

[9] a) L. Zhu, M. Lu, Q. Zhang, D. Qu, H. Tian, *Macromolecules* **2011**, *44*, 4092–4097.

[10] I. A. Banerjee, L. Yu, H. Matsui, *J. Am. Chem. Soc.* **2003**, *125*, 9542–9543.

[11] D. P. Ferris, Y. L. Zhao, N. M. Khashab, H. A. Khatib, J. F. Stoddart, J. I. Zink, *J. Am. Chem. Soc.* **2009**, *131*, 1686–1688.

[12] a) A. Coskun, P. J. Wesson, R. Klajn, A. Trabolsi, L. Fang, M. A. Olson, S. K. Dey, B. A. Grzybowski, J. F. Stoddart, *J. Am. Chem. Soc.* **2010**, *132*, 4310–4320; b) A. Housni, Y. Zhao, Y. Zhao, *Langmuir* **2010**, *26*, 12366–12370; c) D. Liu, W. Chen, K. Sun, K. Deng, W. Zhang, Z. Wang, X. Jiang, *Angew. Chem.* **2011**, *123*, 4189–4193; *Angew. Chem. Int. Ed.* **2011**, *50*, 4103–4107; d) J. Liu, Y. Lu, *J. Am. Chem. Soc.* **2004**, *126*, 12298–12305; e) L. Zhang, Y. Li, D.-W. Li, C. Jing, X. Chen, M. Lv, Q. Huang, Y.-T. Long, I. Willner, *Angew. Chem.* **2011**, *123*, 6921–6924; *Angew. Chem. Int. Ed.* **2011**, *50*, 6789–6792; f) L. Zhu, H. Yan, K. T. Nguyen, H. Tian, Y. Zhao, *Chem. Commun.* **2012**, *48*, 4290–4292.

[13] Y. Inoue, M. Miyauchi, H. Nakajima, Y. Takashima, H. Yamaguchi, A. Harada, *J. Am. Chem. Soc.* **2006**, *128*, 8994–8995.

[14] S.-P. Tang, Y.-H. Zhou, H.-Y. Chen, C.-Y. Zhao, Z.-W. Mao, L.-N. Ji, *Chem. Asian J.* **2009**, *4*, 1354–1360.

[15] a) L. Zhu, X. Ma, F. Ji, Q. Wang, H. Tian, *Chem. Eur. J.* **2007**, *13*, 9216–9222; b) Y. Liu, Y. L. Zhao, H. Y. Zhang, Z. Fan, G. D. Wen, F. Ding, *J. Phys. Chem. B* **2004**, *108*, 8836–8843.

[16] T. Avellini, H. Li, A. Coskun, G. Barin, A. Trabolsi, A. N. Basuray, S. K. Dey, A. Credi, S. Silvi, J. F. Stoddart, M. Venturi, *Angew. Chem.* **2012**, *124*, 1643–1647; *Angew. Chem. Int. Ed.* **2012**, *51*, 1611–1615.

[17] A. Nomura, Y. Sugiura, *Inorg. Chem.* **2004**, *43*, 1708–1713.

[18] T. H. Fife, D. M. McMahon, *J. Org. Chem.* **1970**, *35*, 3699–3704.

[19] R. Breslow, N. Greenspoon, T. Guo, R. Zarzycki, *J. Am. Chem. Soc.* **1989**, *111*, 8296–8291.

[20] H. Wolf, H. Ringsdorf, E. Delamarche, T. Takami, H. Kang, B. Michel, Ch. Gerber, M. Jaschke, H.-J. Butt, E. Bamberg, *J. Phys. Chem.* **1995**, *99*, 7102–7107.

[21] G. H. Woehrle, M. G. Warner, J. E. Hutchison, *Langmuir* **2004**, *20*, 5982–5988.

[22] K. C. Grabar, R. G. Freeman, M. B. Hommer, M. J. Natan, *Anal. Chem.* **1995**, *67*, 735–743.

Received: July 28, 2012

Photoswitchable Catalysis

L. Zhu, H. Yan, C. Y. Ang,
K. T. Nguyen, M. Li,
*Y. Zhao** .... ▮▮▮▮–▮▮▮▮

Photoswitchable Supramolecular Catalysis by Interparticle Host–Guest Competitive Binding

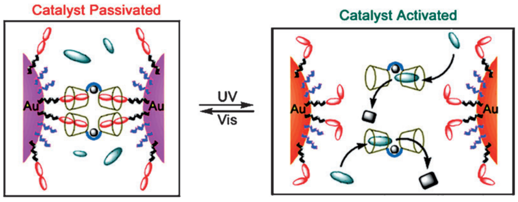

On and off: Ester hydrolysis catalyzed by a Zn^{II}-coordinated β-cyclodextrin dimer can be switched on and off using light in the presence of gold nanoparticles with azobenzene units displayed on their surfaces. Under visible light, the azobenzene units are *trans* and bind tightly to the dimer, thus leading to reduced catalysis. Under UV light, the azobenzene units are *cis* and bind loosely to the dimer, thus allowing substrates to bind and hydrolysis to occur.